



Voltage balancing and synchronization of microgrids with highly unbalanced loads

N.W.A. Lidula^{a,*}, A.D. Rajapakse^{b,1}

^a Department of Electrical Engineering, Faculty of Engineering, University of Moratuwa, Moratuwa 10400, Sri Lanka

^b Department of Electrical and Computer Engineering, University of Manitoba, 75 Chancellor's Circle, Winnipeg, MB, Canada R3T 5V6

ARTICLE INFO

Article history:

Received 3 January 2013

Received in revised form

26 November 2013

Accepted 29 December 2013

Available online 24 January 2014

Keywords:

Frequency and voltage control

Microgrid synchronization

Synchrocheck relay

ABSTRACT

Microgrids can operate in parallel with the grid or as a power-island. They are thus, expected to perform seamless transition from islanded to parallel operation and vice versa. This paper reviews the existing DG interconnection standards for microgrid resynchronization, investigates possible simple solutions for voltage balancing, and shows that the existing synchrocheck relay with a circuit breaker is sufficient to reconnect an islanded, highly unbalanced microgrid back to the utility grid.

© 2014 Elsevier Ltd. All rights reserved.

Contents

1. Introduction	907
2. Review on microgrid synchronization and voltage balancing	908
2.1. Active synchronization	909
2.2. Passive synchronization	910
2.3. Open-transition transfer synchronization	911
2.4. Voltage balancing in microgrids	911
2.5. Summary of review on synchronization and voltage balancing in microgrids	911
3. The microgrid test system	911
4. Microgrid frequency and voltage control	912
4.1. Standards	912
4.2. Microgrid control strategy	912
4.2.1. Synchronous generator control	912
4.2.2. Wind turbine control	913
4.2.3. VSC with PI control	913
4.2.4. Load shedding	913
4.2.5. Switched capacitor bank for voltage balancing	914
5. Analysis of passive synchronization through simulations	914
5.1. Model validation	914
5.2. Role of switched capacitor banks in synchronization	915
5.3. Impact of synchrocheck relay settings	918
6. Conclusions	920
Acknowledgements	920
References	920

* Corresponding author. Tel.: +94 116 503 01x3203; fax: +94 112 650625.

E-mail addresses: lidula@elect.mrt.ac.lk, lidula@gmail.com (N.W.A. Lidula), Athula.Rajapakse@ad.umanitoba.ca (A.D. Rajapakse).

¹ Tel.: +1 480 1403; fax: +1 204-474 7522.

1. Introduction

Historically, power has been provided by centralized generation via transmission lines to regional distribution substations.

With the deployment of clean and efficient energy sources and smart grid technologies, many distributed resources, i.e. distributed generators (DG), energy storage and controllable loads, are now connected to distribution grids. The next logical progression is to allow these sources to provide power for the local load when the traditional grid is not available [1]. This is achieved through microgrids. A microgrid is a portion of an electric power distribution system, formed by distributed generators (DG), energy storage and loads, with the ability of operating in parallel with grid or as a power island. Microgrid is an attractive structure to harness the reliability benefits offered by DGs [1–3], and it has been a subject well researched around the world in the recent past [4]. The benefits of microgrids were well recognized after the super storm Sandy that devastated the electricity supply across a number highly populated areas in the North America [1]. The key to reap the benefits of microgrids is in the ability of smoothly change from parallel operation to autonomous operation and vice versa. The newly introduced IEEE STD 1547.4-2011 *Guide for Design, Operation, and Integration of Distributed Resource Island Systems with Electric Power Systems* [5], addresses the issue of intentional islands, which was missing in the IEEE STD 1547-2003 [6] for *Interconnecting Distributed Resources with Electric Power Systems*. The IEEE standards on interconnection of distributed resources have been the basis for interconnection regulations or guidelines of many power utilities worldwide.

Except for the microgrids in isolated areas, microgrids are typically interconnected to the traditional grid. When the traditional grid supply is disrupted, the microgrid becomes an autonomous entity operating in islanded mode. The microgrid needs to be reconnected to the traditional grid when it is restored. This is the main subject that is discussed in this paper. When reconnecting a microgrid operating in the islanded mode to the utility grid, voltage, frequency and phase criteria must be satisfied. Synchronizing a microgrid having several generators with different characteristics is more challenging than synchronizing a single generator with the grid. In [5], three methods of synchronization have been identified: (i) active synchronization where there is a control mechanism to match the voltage, frequency, and phase angle of the island system to the utility grid, (ii) passive synchronization, which employs a synchronization check for parallel-

ing, and (iii) open-transition transfer where loads and DGs in the island are de-energized before reconnecting to the grid.

Active synchronization is an attractive method, especially for converter based distributed resources. However, active methods have special infrastructure requirements such as dedicated communication facilities. Open transition method lowers the reliability benefits as it requires interruption of the loads before reconnecting the microgrid with the utility grid. Among the three methods, passive synchronization is a simple method that does not require special control mechanisms or temporary interruption of loads. The technology of synchrocheck relays used for passive synchronization is well established and therefore it is attractive for practical application. However, there is lack of information on any limitations that may encounter in applying this method to practical microgrids which may have poor voltage and frequency control capabilities. Aim of this paper is to review the various methods proposed for synchronization of microgrids, and explore the performance of a synchrocheck relay in synchronizing a highly unbalanced microgrid whose frequency is controlled using a synchronous generator.

2. Review on microgrid synchronization and voltage balancing

The IEEE STD 1547.4-2011 [5] has a brief discussion on microgrid synchronization. The standard recommends that in order to initiate a reconnection of an islanded microgrid and the utility grid, the voltage of the utility grid should be within the “Range B of ANSI/NEMA C84.1-2006, Table 1” and the frequency range should be between 59.3 Hz and 60.5 Hz (for a system of 60 Hz nominal frequency), and phase rotation must be correct. Further, the voltage, frequency, and phase angle between the islanded microgrid and the utility grid should be within acceptable limits specified in the IEEE STD 1547-2003 [6]. The IEEE STD 1547.4-2011 [5] recommends ensuring the stability of the utility grid by delaying the reconnection of the islanded microgrid for up to five minutes after the steady-state voltage and frequency of the utility grid are restored to the recommended ranges. Synchronizing methods as categorized in [6] are discussed below presenting the relevant literature under each category.

Table 1
Summary of different features of microgrid synchronization techniques and their applications.

Synchronization approach	Approach [4]	Complexity and power reliability	Economy	Applications	Examples
Active	There is an inbuilt control mechanism to match the voltage, frequency, and phase angle of the island system to the utility grid	<ul style="list-style-type: none"> Complex controlling techniques involve Maintain the power reliability 	<ul style="list-style-type: none"> Comparatively high capital cost Depends on the Technique 	Mostly applied for inverter based systems, but can be applied in hybrid systems	<ul style="list-style-type: none"> CERTS microgrid Test-bed—United States [27] Test microgrid at Akagi of the CRIEPI – Japan [28] Sendai project – Japan [29]
Passive	Employs a synchronization check for paralleling	<ul style="list-style-type: none"> Existing simple synchronization technologies can be used Maintain the power reliability 	<ul style="list-style-type: none"> Lower capital cost compared to active synchronization methods 	For synchronous generator based systems or hybrid systems having different types of generation	<ul style="list-style-type: none"> Boston Bar microgrid—BC Hydro, Canada [30]
Open-transition transfer	Loads and DGs in the island are de-energized before reconnecting to the grid	<ul style="list-style-type: none"> Simple Reduces the power reliability 	<ul style="list-style-type: none"> No capital cost Incurs loss of revenue with low power reliability 	For inverter based, synchronous generator based or hybrid systems	<ul style="list-style-type: none"> Boralex planned islanding—Hydro Quebec (HQ), Canada [30]

Fig. 1. Schematic diagram to illustrate active synchronization.

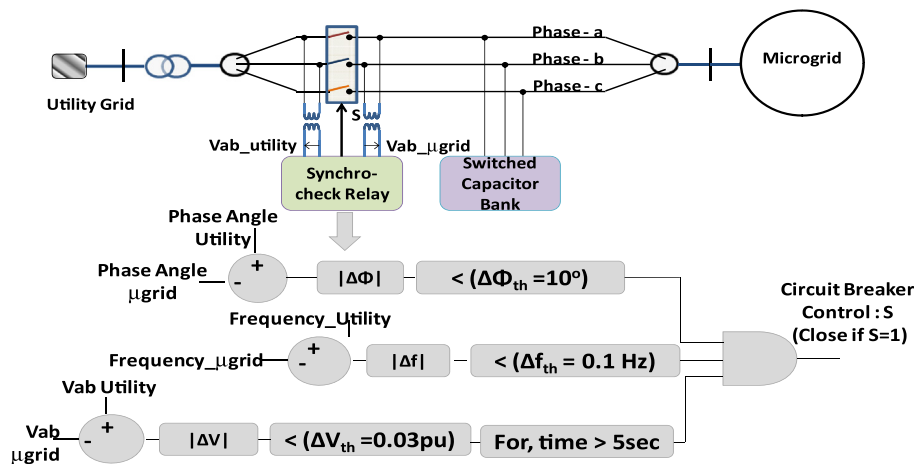


Fig. 2. Microgrid synchronizing function in accordance with [6].

proposed in [12]. The proposed grid synchronization method adjusts the Distributed Energy Resources Controls (DERC) operation frequencies and phase angles through the frequency restoration of the $P-\omega$ droop control. DERCs' output voltage magnitudes are altered through the voltage restoration of $Q-V$ droop control. Because of the proportional sharing of real power and the reactive power there are negligible transients in the process of synchronization. The methodology is validated by simulation and using a pilot microgrid setup having converter based DG.

A three-level hierarchical control for AC and DC microgrids having converter based DGs is proposed in [13]. The primary control deals with the inner control of the DG units to control their output impedances while the secondary control restores the frequency and amplitude deviations produced inside the microgrid providing an active synchronization technique. The tertiary control regulates the power flow between the grid and the microgrid at the point of interconnection.

In [14], a control algorithm based on the adaptation of a dual second-order generalized integrator based on a frequency-locked loop is proposed for controlling the disconnection and resynchronization of converter based microgrid. Using the frequency detection by the frequency-locked loop, the synchronization and the current and voltage control loops are implemented in the $\alpha-\beta$ stationary reference frame. The proposed methodology is an active synchronization technique.

Use of a modified voltage based droop control for active synchronization in converter based microgrids is presented in [15]. The voltage at the point of interconnection is measured and communicated to the synchronizing DG unit that uses a phase-locked-loop to obtain the rms voltage and its phase angle. A sufficiently large, dispatchable DG close to the point of interconnection is selected for the synchronization of the microgrid. The paper proposes to modify the voltage based droop controller of the synchronizing unit by including an rms voltage synchronization block, a droop limiting block and a phase synchronization block. The voltage, phase angle and frequency of the synchronizing DG are controlled to their respective values at the point of interconnection.

A methodology based on phase locked loop (PLL) to synchronize the phase and frequency of a centralized microgrid with the electrical distribution network is presented in [16]. It uses three different PLL structures, based on a second-order linear and time-invariant observation model, which provides a real-time angle and frequency estimation with a negligible delay. The signal synchronization is obtained by means of the 1 Pulse Per Second (1 PPS) signal, provided by any GPS devices, in order to generate a common timing reference for each Distributed Energy Resource Unit connected to the Microgrid.

2.2. Passive synchronization

Passive synchronization methodologies also require sensing of the system conditions of both utility and the islanded microgrid as they employ a synchronization check in the microgrid paralleling device. The synchronization check is generally achieved using a synchrocheck relay.

The synchrocheck relay is a device which measures the magnitude, phase angle and frequency differences between the voltages on either side of the circuit breaker. The relay allows the circuit breaker closing only if the measured values are within some preset limits. These limits are set based on the synchronization requirements given in [6,17] for DG interconnection. Generally, the synchrocheck relay measures the line voltage taking only two phases and the existing synchrocheck relays utilizes zero-crossing technique to find the phase angles [18,19]. A schematic diagram of the synchrocheck relay is given in Fig. 2. Passive synchronization techniques may take longer to reconnect than the active synchronization methods.

The synchronization study reported in [20] is a passive synchronization approach. Further, it has considered converter based DGs as well as synchronous generators. It concludes that with the use of PLLs in converter based DGs, resynchronization is not an issue if phase difference across the interconnection switch is small (less than 10°) when there are only converter based DGs in the microgrid. The paper [20] further states that with the synchronous generator, even a small phase difference existing across the interconnection switch during reconnection could be problematic, and emphasizes the requirement for solutions to minimize the phase angle difference and to balance the voltages to facilitate smooth transition.

In [21] a synchronization method for a small hydro generation based medium voltage microgrid situated in Brazil, is proposed. Although, some elements of active synchronization such as communication links are present, this methodology is basically a passive synchronization technique. Once the main system has been restored, the operator at the distribution substation sends a command to close the circuit breaker and to the DG to activate synchronization control system through a dedicated communication channel connected between the small hydro plant and the distribution substation. The circuit breaker closing is activated only if the minimum parallelization conditions that will be verified by the synchronism check relay are met. Frequency and voltage at both sides of the coupling circuit breaker are measured and sent to the distributed generator (DG) unit. Based on frequency and voltage mismatches, the synchronization control system, located at the DG site, responds with additional signals to the speed and

voltage regulators, respectively. The automatic voltage regulator acts to change the field voltage and reduce the voltage error between the two islands. If the synchronization mode is active, the frequency mismatch is used as an additional signal to the turbine to control the speed. In order to guarantee the possible reconnection, a small frequency error is intentionally introduced.

2.3. Open-transition transfer synchronization

The open-transition transfer synchronization method merely de-energizes the loads and the DGs in the microgrid before reconnection. Although, this methodology is technically sound in the utility perspective, it reduces the level of reliability of the system.

2.4. Voltage balancing in microgrids

Since many single phase loads are connected to distribution grids, voltages unbalances exist in practical microgrids. Unbalance voltages can pose difficulties in achieving the synchronization criteria, especially with respect to voltage and phase angles limits. When a severe voltage unbalance exists, aid of a voltage balancing scheme may be required to perform successful synchronization. There are number of approaches proposed for voltages balancing in microgrids including (i) introduction of special control loops to converter based DGs and energy storage units, (ii) using reactive support devices such as SVC's or D-STATCOMs with appropriate control, and (iii) use of simple switched capacitors.

The use of switched capacitors for voltage balancing is simple. Capacitors are switched-in in stages if the phase voltage drops below a set value, generally after a certain time delay. The time delays for each stage are selected inversely proportional to the difference between the nominal voltage and the threshold voltage for the stage. Sometimes, capacitor switching is blocked if the frequency is deviated from the nominal to avoid unnecessary switching transients. Application of switched capacitors for voltage balancing in a microgrid has been investigated in [20].

Voltage balancing in converter based microgrids having single-phase and three-phase loads is discussed in [22]. A controller for voltage balancing is proposed. The controller sets the d -axis and q -axis components of the negative sequence current to regulate the negative sequence component of the collector bus voltage vector to zero, achieving the balance.

Use of linear-quadratic regulator for voltage control in converter based microgrids is discussed in [23]. Based on the measurements of voltage at the point of interconnection, the desired grid voltage is tracked by using a linear-quadratic regulator. It is stated that the linear-quadratic regulator shows good tracking performance and has low parameter sensitivity.

In [24], a droop control method for voltage balancing is proposed. The proposed methodology is applicable only to converter based microgrids. The negative sequence voltage references are drooped against the negative sequence output currents. Therefore, voltage source converters in parallel compensate for the voltage imbalance and jointly share the negative sequence currents in proportion to a predetermined ratio regardless of the plant parameters.

Use of D-STATCOM for voltage balancing is discussed in [25]. The D-STATCOM operates as a conductance at the fundamental positive-frequency to restore the positive-sequence voltage to the nominal value and it operates as a separate conductance at the negative-sequence frequency to suppress the negative-sequence voltage to an allowable level. The conductance commands are dynamically tuned according to voltage fluctuation at the installation location, so voltage variation could be reduced in response to load change and variable renewable energy.

In [26], design of low power, prototype model of a Static Var Compensator (SVC) for voltage regulation in microgrids is

presented. The SVC is designed to compensate variations of the line voltage of a microgrid in a range of $\pm 2\%$. The developed SVC is capable of operating in a grid with a rated line voltage of 400 V.

2.5. Summary of review on synchronization and voltage balancing in microgrids

Table 1 differentiates each synchronization technique on complexity, cost and applications. A detailed literature review by the authors on experimental microgrids [3] presents the control technologies adopted in implemented microgrids around the world. Some of the literature reviewed in [3] reports the synchronization technique applied, and they are also listed in Table 1 as examples of adopting different synchronization techniques.

Among the numerous published research on islanded and parallel operation of microgrids, there are only few studies which specifically study the subject of microgrid synchronization. Most literature among them are focused on inverter based DGs and there is lack of comprehensive study on the applicability of DG interconnection standards for microgrid synchronization [5]. Table 1 show that active synchronization is more commonly applied on the implemented microgrids. It is evident from literature that active synchronization techniques have been improved to ensure stable transition from islanded to grid connected operation through continuous research and development [7–11]. Many microgrids are implemented as demonstration projects, and they tend to implement inverter based DGs and new active synchronization techniques as part of the technology demonstration. Although, passive synchronization is simpler and more cost effective in comparison to active synchronization, there is general lack of published experience on the adequacy or any potential issues with passive synchronization of microgrids. Literature survey also indicates that similar to the work on synchronization of microgrids, most of the research on voltage balancing of microgrids is focused for converter based systems. Therefore, rest of this paper focuses on reporting the issues and challenges of passive synchronization of synchronous generator based microgrids with highly unbalanced loads using commercially available synchrocheck relays [17]. Simple switched capacitor banks are considered for voltage balancing at the point of interconnection to support the synchronization process.

This paper considers a microgrid with a synchronous generator, an induction generator, and an inverter based DG, in contrast to [7–11,20,22–24]. Using time domain simulations, the paper analyses the impact of applying existing DG synchronization standards [6], as suggested in [5], to a typical medium voltage microgrid with unbalanced loading. The DG interconnection guidelines of a local utility is [17] also considered.

3. The microgrid test system

The test network shown in Fig. 3 is a medium voltage (MV) microgrid derived from the proposed CIGRE MV benchmark test system [31]. The system was originally developed for DG interconnection studies based on an actual power system. It was augmented with the features necessary for microgrid operation after an extensive review of microgrid research [4].

To emulate a generic microgrid [4], three different sources of DGs were integrated. A 3 MW steam turbine driven synchronous generator is connected to bus-10, a 1 MW wind turbine driven fixed speed induction generator is connected to bus-7 with a 0.5 MVar of capacitive compensation, and a 0.35 MVA DC source (representing a photovoltaic (PV) system) is connected to bus-3 via a VSC. The high capacity DG (the synchronous generator) was used to avoid the necessity of an energy-storage [4]. One distinct

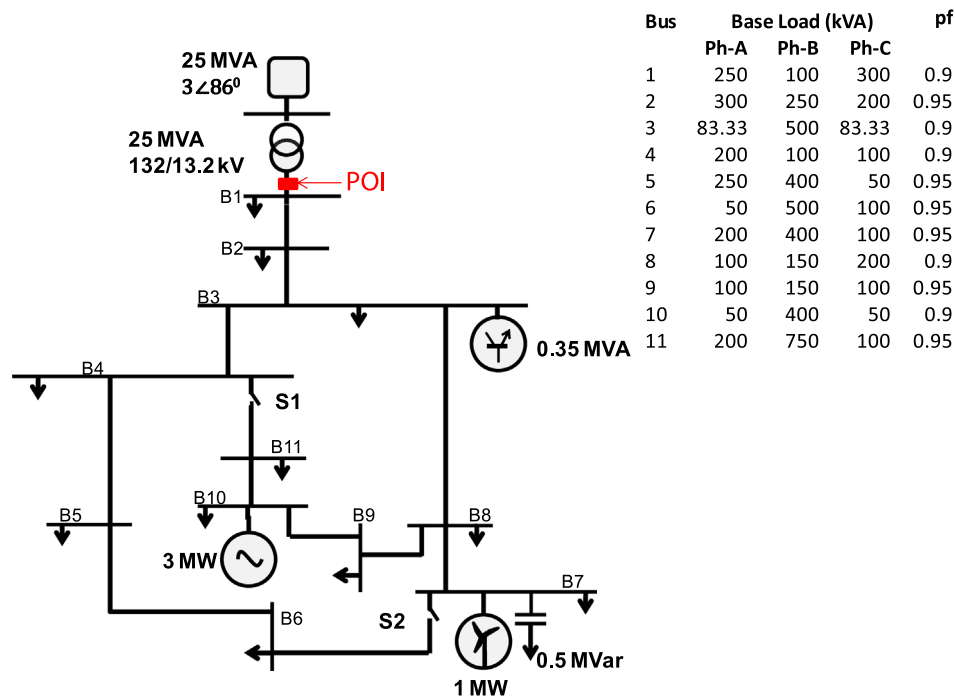


Fig. 3. Microgrid test system.

Table 2
Standards for DG synchronization [17].

Total generation (KVA)	Frequency difference (Hz)	Voltage difference (%)	Phase angle difference (°)
0–500	0.3	10	20
> 500–1500	0.2	5	15
> 1500	0.1	3	10

feature of this test network is that the loads are highly unbalanced, with Phase-b having the greatest load.

Generally, loads are evenly distributed on all three phases based on the nominal ratings, but unbalanced situations can occur during the operation depending on the actual power drawn by the loads at a given time. All loads in the network were simulated as constant $R-L$ loads. Part of the loads was considered as controllable [4]. Microgrid interconnection relay and the switched capacitor bank are connected at the point of interconnection (POI). In order to meet the operational and synchronization requirements during the islanded operation, this microgrid is equipped with an automatic load shedding scheme to control the frequency, and an automatic capacitor switching scheme for voltage balancing. The two switches S1 and S2 are normally kept open. Simulation studies were carried out using PSCAD/EMTDC power system simulation software [32].

4. Microgrid frequency and voltage control

4.1. Standards

A microgrid should maintain the power quality requirements during both parallel and islanded operation. The guidelines in [5] refer to the power quality limits defined in the DG interconnection standards [6]. In this paper, guidelines of the local utility outlined in, “Technical requirements for connecting distributed resources to the Manitoba Hydro distribution system” [17], was used in studying the microgrid control and synchronization performance.

Manitoba Hydro has used the IEEE STD 1547-2003 [6] as the basis for its interconnection guidelines.

According to [17], the steady state voltage operating range for distribution systems above 1 kV is $\pm 6\%$, and the normal system frequency range is ± 0.2 Hz. The voltage unbalance, as defined in (1), is expected to be below 4% in urban areas under normal operating conditions [17].

$$\text{Voltage Unbalance (\%)} = \frac{\Delta V_{\max}}{V_{\text{avg}}} \times 100 \quad (1)$$

In (1) V_{avg} is the average of the three phase voltages and ΔV_{\max} is the maximum deviation from the average phase voltage. The specific requirements that need to be satisfied in reconnecting a DG to the system are shown in Table 2 [17]. The guidelines in [17] specifically states that the DG must be reconnected only after the system has stabilized and the RMS voltage has returned to normal levels for a minimum of 5 min. This requirement is in agreement with [6]. The standards applied for DGs rated above 1500 kVA are considered applicable to the microgrid as a whole.

4.2. Microgrid control strategy

An agent based control mechanism was considered in this study. The management agent is responsible for operation planning, load shedding/restoration, monitoring and microgrid synchronization. The communication agent carries the status of each local agent to and from the management agent. The operating point of each DG is assigned by the management agent as part of operational planning. Islanding detection is a responsibility of the generator local agents, and it is assumed that islanding events are detected within 50 ms using a fast islanding detection method [4,33,34].

4.2.1. Synchronous generator control

The steam turbine driven synchronous generator emulates a co-generation plant. Standard synchronous generator and steam turbine models available in PSCAD/EMTDC are used with typical parameter values obtained from [35]. The standard IEEE alternator

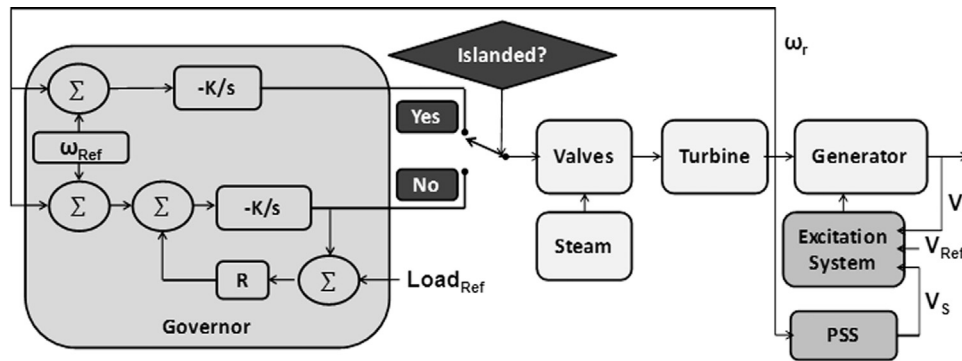


Fig. 4. Synchronous generator with frequency and voltage control.

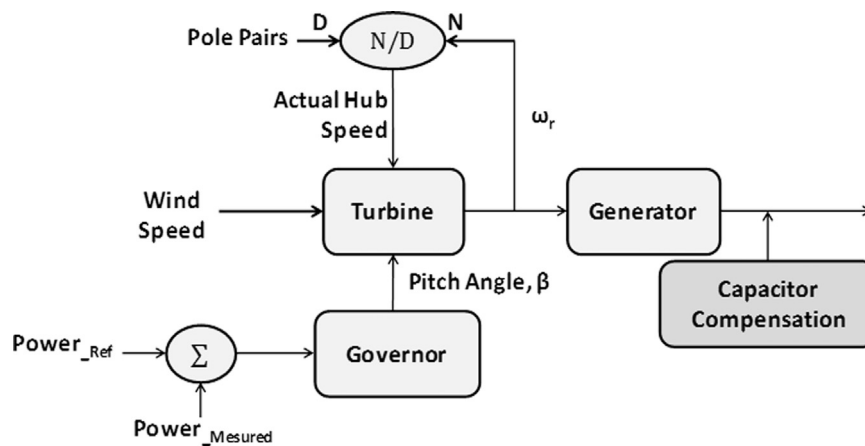


Fig. 5. Block diagram of wind farm.

supplied rectifier excitation system (AC1A) is used for voltage control and a power system stabilizer (PSS) is also incorporated to improve the system damping. An electro-hydraulic controlled governor excluding the over speed control is used for frequency control [35]. A simple block diagram of the system is shown in Fig. 4.

In the grid connected operation, synchronous generator is run as a constant PV generator, and it is in droop control mode, with 5% droop and with typical time constants [35]. In the islanded mode, the synchronous generator is run as an isochronous generator. In this mode, the droop setting is made nearly equal to zero, effectively changing the governor to constant frequency operation. The output power of the synchronous generator will change to follow the variations in the load demand while maintaining constant frequency.

4.2.2. Wind turbine control

The block diagram of the wind generator is shown in Fig. 5. The modeled wind turbine drives a fixed speed induction generator and it is integrated with a pitch control mechanism to control the output power. A 0.5 MVar capacitor bank is connected at the generator terminal for reactive power compensation. The initial pitch angle (β) is found as suggested in [36] by calculating the power coefficient to give 0.6 MW constant power output at a wind speed of 12 m/s. Thus, the corresponding initial pitch angle is 14.2°.

4.2.3. VSC with PI control

The DC source interconnected via a VSC represents the interface of a solar PV system. It is equipped with typical VSC components [37] such as the DC capacitor, and an extra AC phase reactor (to reduce harmonics in AC currents). Considering the

highly unbalanced nature of the microgrid, the VSC system is connected to one of the stronger buses (closer to POI and synchronous generator). Since the simple decoupled control of VSC is not possible due to the unbalanced nature [38], direct control of VSC is used. The direct control involves adjusting the modulation index and the phase angle of the sine-wave pulse width modulator (SPWM) directly according to the parameters being controlled [37]. A phase locked loop is used in the SPWM for firing control.

The VSC is allowed to regulate the bus voltage under both parallel and islanded operation of the microgrid. Its real power output is controlled by a simple PI controller that adjusts the phase angle of the SPWM to maintain the DC bus voltage at a reference value. Similarly, a PI controller is designed to control the voltage after the interconnecting transformer. The terminal voltage error is minimized by adjusting the modulation index of the SPWM. The initial parameters of the PI controllers are found by trials and later optimized using simplex method using the optimization tools available in PSCAD/EMTDC [39].

4.2.4. Load shedding

When the microgrid is islanded, a fast load shedding scheme is automatically activated to restore the balance between the load and available generation, and thereby prevent the frequency collapse [4]. The static and dynamic under-frequency load shedding are the two most widely applied concepts [40–43]. Although, dynamic load shedding, which determines the amount of load to be shed at each stage by considering the magnitude of generation loss and available load on each feeder [41] is conceptually superior, static load shedding schemes are more common in practical power

systems due to its simplicity [40,42,43]. Therefore, a static load shedding scheme is used here.

In the advanced static load shedding schemes, both frequency and rate of change of frequency (ROCOF) is fed into the controller and when the frequency goes below a preset value, and if the rate of change of frequency is more than a pre-set value, the controller initiates a signal to trip the loads assigned priority 1 (stage 1). If the frequency goes further down, the next stage of loads will be dropped and this will continue until the frequency stabilizes to its nominal value. Priorities are assigned to the loads at the design stage, considering their relative importance and the normal loading. However, in static load shedding, the real load behind the breaker or how much load has to be shed in order to reestablish the load balance is generally unknown [40,41].

Designing a static load shedding scheme involves four main steps [40]: (i) Calculation of total load to be shed, (ii) deciding the number of load shedding stages and the size of load to shed at each stage, (iii) setting the frequency and rate of change of frequency thresholds, and (iv) setting the time delays. The final load shedding scheme designed for this microgrid is shown in Fig. 6. The settings were found with the help of simulation studies. To avoid system collapse due to slow frequency drifts, time delayed back up relays, which operates regardless of the initial rate of change of frequency, are provided at each stage of the load shedding scheme.

4.2.5. Switched capacitor bank for voltage balancing

One aspect studied in this paper is the use of switched capacitors for voltage support/balancing in a microgrid with unbalanced loads.

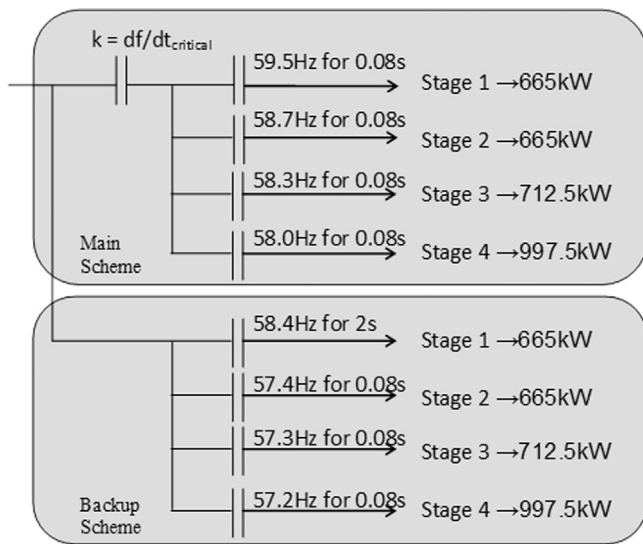


Fig. 6. Schematic representation of the designed load shedding scheme.

The capacitor bank is designed based on commercially available capacitor units considering their ratings and switching logics [44,45].

The capacitor bank connected at the POI of the microgrid consists of three parallel units and single pole switching is used for voltage balancing. Capacitors are switched-in depending on the measured phase voltages; i.e. if the phase voltage drops below the set value for duration greater than a specified time delay, the appropriate capacitor is connected to the system [44]. In order to minimize transients, capacitor switching is initiated only if the frequency is within ± 0.1 Hz from the nominal. Time delays for each stage are selected inversely proportional to the difference between the nominal voltage and the threshold voltage for the stage. Fig. 7 shows the arrangement of the three-stage voltage balancing capacitor bank rated at 150 kVar/phase/stage.

5. Analysis of passive synchronization through simulations

Simulation studies are carried out with the assumption that the initial operating points of the generators are already set by the management agent. Therefore, it is considered that the power output of synchronous generator, VSC based source and the wind turbine are at 0.9 pu, 1 pu and 0.6 pu respectively at the time islanding happens for all the simulations. The inertia constant of the wind turbine generator and the synchronous generator are 0.5 s and 3 s, respectively.

5.1. Model validation

To validate the accuracy of the model, microgrid is islanded at $t=2$ s while the microgrid is operating parallel to the grid at its base load. The variations of the power, frequency and the voltage during the islanding event are shown in Fig. 6. When the microgrid is islanded, the synchronous generator switches to isochronous mode, bringing back the frequency to nominal value. The frequency reference is set to 1.00045 pu, with the intension of facilitating resynchronization when the utility grid is restored. VSC based DC current source is still operated as constant PV generator, while the wind farm is run as a constant PQ generator. Since there is a power deficit in the islanded microgrid, the load shedding scheme should be activated. The switched capacitor bank is intentionally blocked in this simulation. The *power imbalance* in the microgrid at a transition is defined as the grid power being lost as a percentage of the total power consumption. This is computed using (2).

$$P_{\text{imbalance}} = \frac{\pm P_{\text{Grid}}}{(P_{\text{Grid}} + P_{\text{Synch}} + P_{\text{Wind}} + P_{\text{VSC}})} \times 100 \quad (2)$$

Fig. 8(a) and (b) presents the active and reactive power responses of each source for the islanding event corresponding

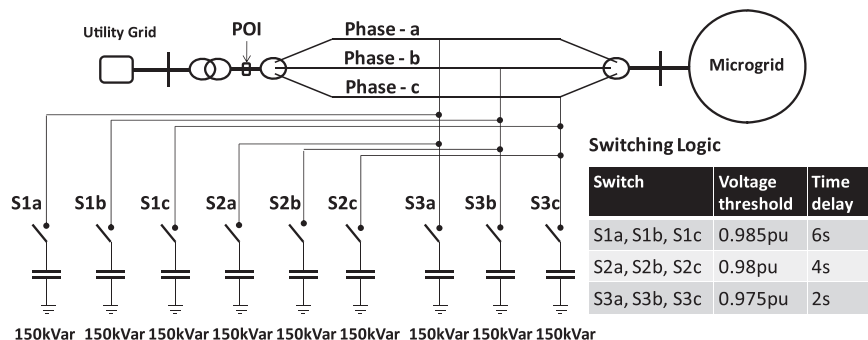


Fig. 7. Switched capacitor bank for voltage balancing in the microgrid.

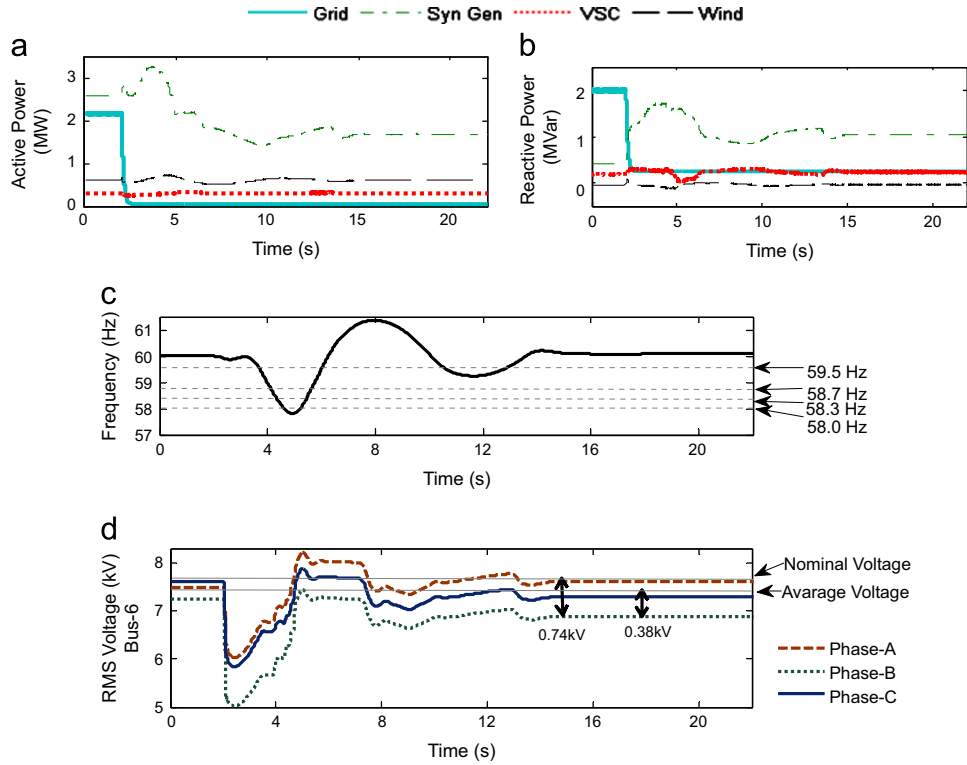


Fig. 8. (a) Active power (b) reactive power (c) frequency, (d) terminal rms voltage at the Bus-6 to an islanding of at $t=2$ s (40% power imbalance).

to a +40% power imbalance. The synchronous generator stabilizes the frequency after islanding, while the other two sources operating as constant power sources.

The frequency response of the microgrid for the islanding event is shown in Fig. 8(c). The frequencies at which the loads are shed are marked by horizontal lines. Load shedding scheme undergoes all four stages to stabilize the frequency. Islanded operation satisfies the expected frequency standards having the deviation within 0.1 Hz.

Fig. 8(d) presents the variation of terminal voltages of Bus-6, which is the weakest (in the sense that furthest from the POI and no DG support). In the parallel operation of the microgrid, Phase-b shows the highest voltage deviation from the nominal and it is around -4.9%, and the maximum voltage unbalance calculated using (1) is 2.7% for this operating condition. It confirms that the microgrid parallel operation at the base load satisfies the frequency and voltage standards without any reactive power support from the capacitor bank. Phase-b indicates the lowest voltage levels in the islanded operation as well. The maximum voltage deviation in islanded operation from the nominal is around -9.73%. Thus, it is higher than the allowable voltage deviation ($\pm 6\%$ maximum). The maximum voltage unbalance observed in the islanded operation is around 5.24%, which is also greater than the expected standards (4%).

The above observations confirms that the modeled microgrid test system performs accurately as designed. However, voltage quality of the microgrid needs to be improved during the islanded operation and for resynchronizing the microgrid back to the utility grid.

5.2. Role of switched capacitor banks in synchronization

The requirements for synchronization of a DG with Manitoba Hydro's grid, outlined in Table 2, are applied to synchronization of the microgrid, and thus the synchrocheck relay settings should be as indicated on the logic diagram shown in Fig. 2. The nominal

voltage and frequency of the microgrid at POI is 13.2 kV, 60 Hz. A circuit breaker time delay of 83 ms [45] is introduced to emulate the practical scenario.

In order to examine the effect of capacitors on voltage, first an islanding event is simulated. Just before the islanding, microgrid was importing 40% of the real power from the utility grid (+40% power imbalance). Fig. 9 shows the variations of phase angle difference across the breaker, as well as the frequency, and line voltage magnitudes measured on either side of the circuit breaker. Variations are shown with and without the switched capacitor bank at the POI. When islanded at $t=5$ s, first the load shedding scheme is activated to stabilize the frequency. In the case of microgrid equipped with switched capacitor bank, capacitors are then switched-in according to the set logic to correct the voltage levels.

Fig. 9 also gives the highest values observed in the phase angle, frequency, and voltage differences, as well as the highest voltage deviation and voltage unbalance observed during the stable islanded operation under both scenarios. It is clear from Fig. 9 that the voltage magnitude difference requirement for synchronizing ($\Delta V < 0.03$ pu) is not met if the microgrid is operated without the switched capacitor bank. Introduction of the switched capacitor bank not only raised the voltage to a value that meets the synchronization requirements, but also reduced the maximum voltage deviation from -9.73% to -4.74%, and the voltage unbalance from 5.24% to 1.85%.

Fig. 10 shows the simulation results for reconnecting the islanded microgrid back to the utility. Prior to the reconnection, the microgrid operates in the islanded mode as result of an islanding event that resulted in a +40% power imbalance. Thus, this can be considered as reconnection after the islanding event shown in Fig. 9. Fig. 9(a) and (b) shows the grid side instantaneous current and the power outputs of all the sources, respectively. Fig. 10 shows these results for three scenarios: Scenario 1—forced reconnection of the microgrid to the utility grid at a phase angle deviation of 20° ($\Delta\phi=20^\circ$) without the switched capacitor bank,

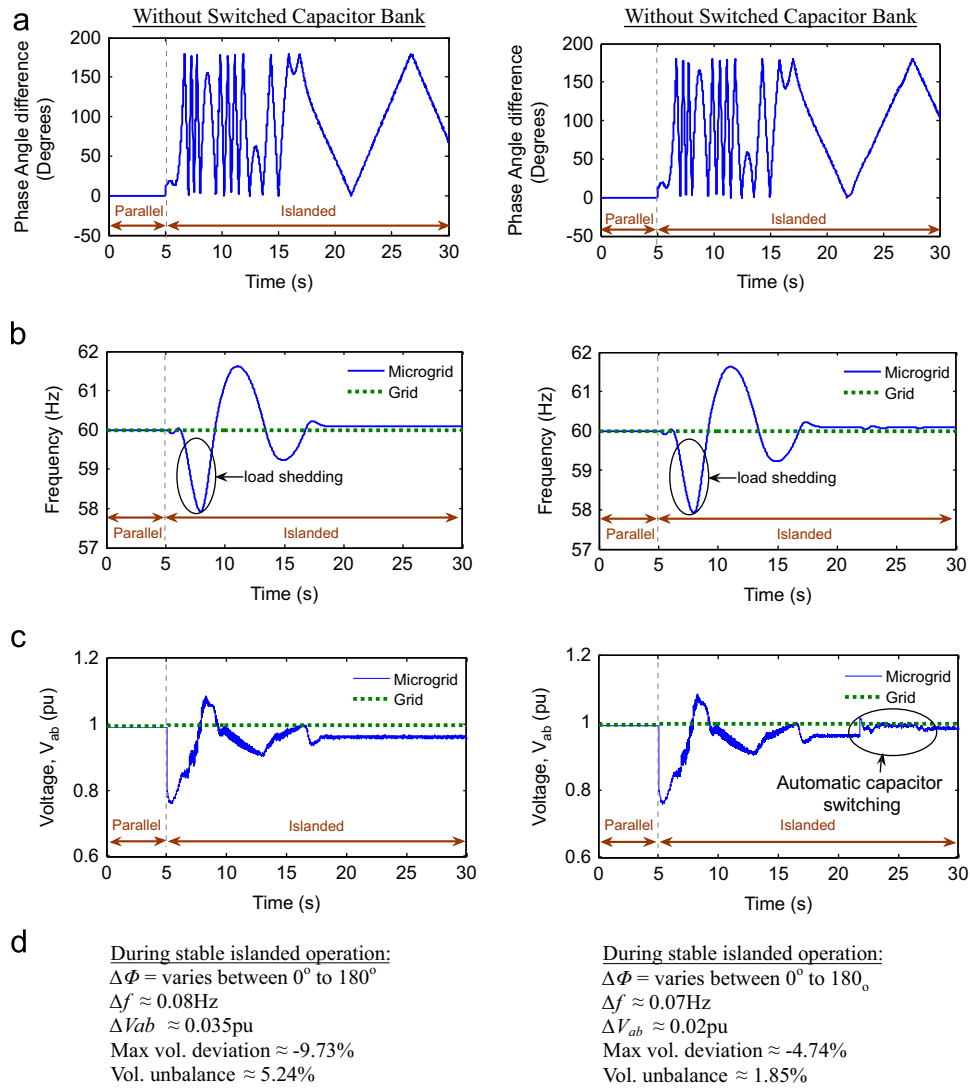


Fig. 9. (a) Phase angle difference, (b) frequency, (c) V_{ab} beside the circuit breaker, (d) summary for an islanding at $t=2$ s (40% power imbalance).

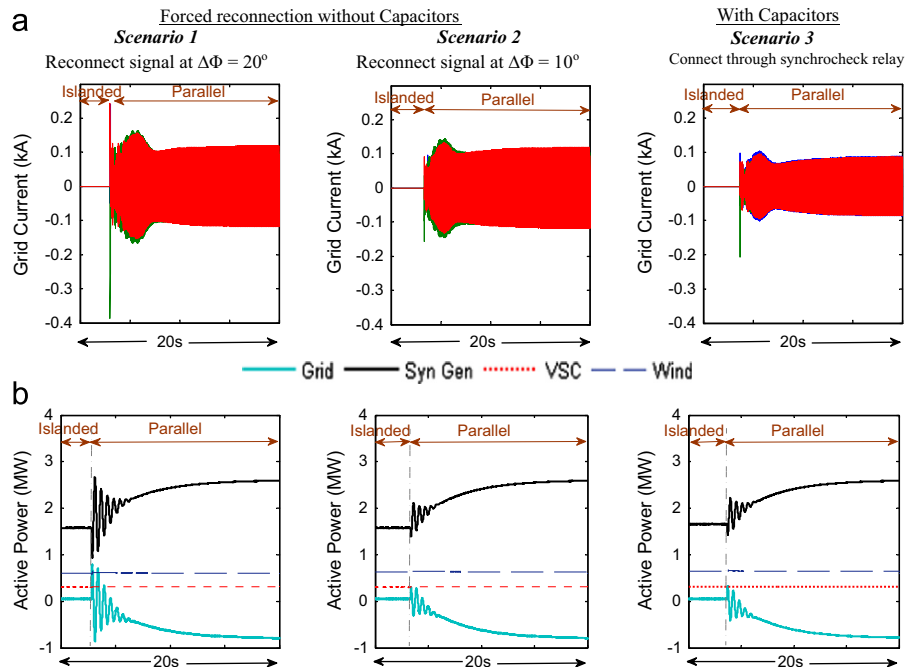


Fig. 10. (a) Grid current, (b) power outputs of all sources at a reconnection of microgrid to utility after an islanding of 40% power imbalance.

Table 3
Voltage regulation with switched capacitors.

Power imbalance (%)	Max voltage deviation at bus-6		Voltage unbalance	
	No capacitors (%)	With capacitors (%)	No capacitors (%)	With capacitors (%)
40	−9.73	−4.74	5.24	1.85
−7	−9.50	−5.40	5.95	3.60

Table 4
System conditions at the time of reconnecting.

Power imbalance (%)	Detail	Forced reconnect without capacitors		With capacitors
		Scenario 1 Reconnect signal at $\Delta\phi=20^\circ$	Scenario 2 Reconnect signal at $\Delta\phi=10^\circ$	Scenario 3 Connect through synchro. relay
+40	$\Delta\phi$	17.28°	7.56°	7.56°
	Δf	0.08 Hz	0.08 Hz	0.07 Hz
	ΔV_{ab}	0.035 pu	0.032 pu	0.02 pu
−7	$\Delta\phi$	18.36°	9.72°	9.72°
	Δf	0.06 Hz	0.06 Hz	0.05 Hz
	ΔV_{ab}	0.045 pu	0.04 pu	0.005 pu

Scenario 2—same as Scenario-1 but $\Delta\phi=10^\circ$, and Scenario 3—reconnection using synchrocheck logic in Fig. 3 with the support of switched capacitors to meet the voltage criteria. Note that, the voltage condition for synchronization cannot be met without the capacitor bank support (Fig. 9).

Aforementioned study was repeated for reconnecting the microgrid back to utility after an islanding event that created a −7% power imbalance (microgrid was exporting power to the grid before the islanding event). In this case also, the islanded microgrid was not able to satisfy the voltage standards without switched capacitor support. The voltage regulation and balancing achieved with the support of switched capacitors at POI of microgrid is summarized in Table 3 for microgrid islanded operation at both +40% and −7% power imbalances. Table 3 shows that even though the capacitor bank is connected only at the microgrid POI, the weakest Bus (Bus-6) voltage is improved by nearly 5% and the voltage unbalance in the islanded microgrid is reduced by nearly 3%.

Despite having very different system condition, variations of the voltage and current during the synchronization at −7% power imbalance case (not shown) is very similar to those observed in the case of +40% power imbalance, shown in Fig. 10. Table 4 summarizes the system conditions at the time of reconnecting the microgrid to utility grid, for the six cases.

Table 4 shows that, the voltage criterion for synchronization cannot be satisfied without the switched capacitors. If the microgrid is forcefully reconnected to the utility grid with a signal initiated at a phase difference of 20° , (both voltage and phase angle criteria are violated) current transient that has a peak

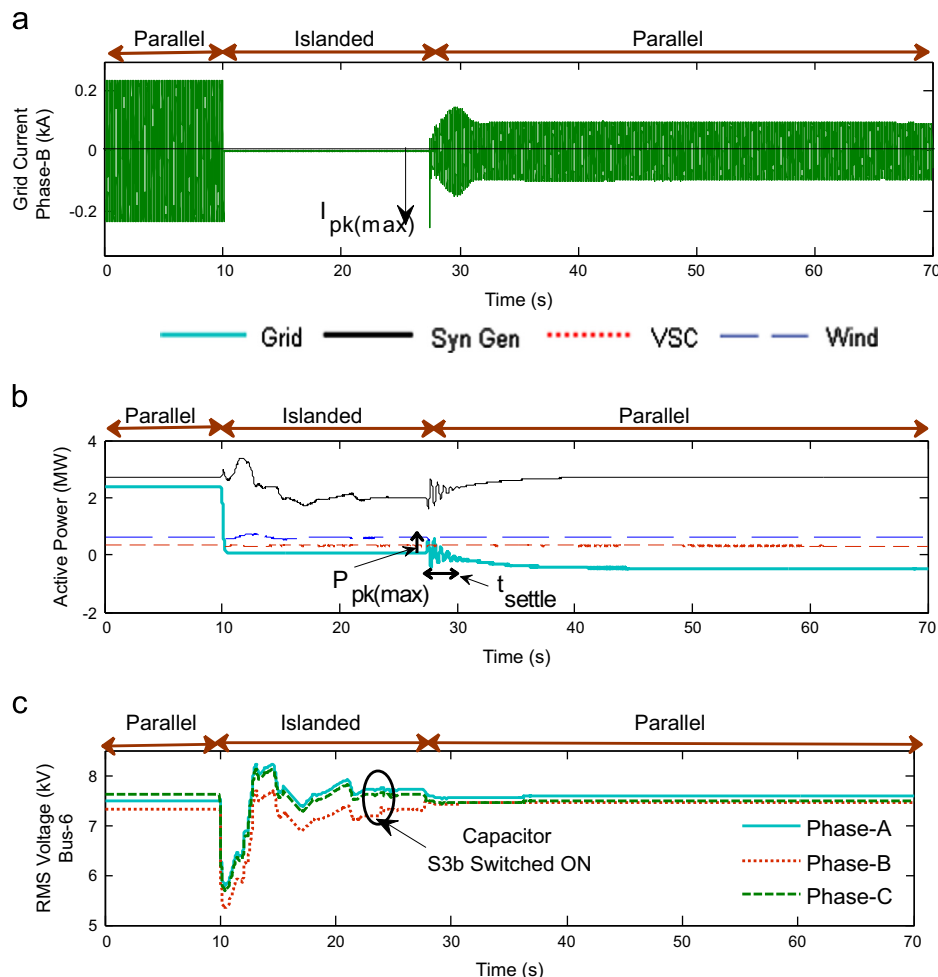


Fig. 11. (a) Grid Ph-bcurrent, (b) utility/DG real power (c) RMS voltages of Bus-6 (+40% power-imbalance, $\Delta V_{th}=0.05$ pu, $\Delta\phi_{th}=10^\circ$, $\Delta f_{th}=0.1$ Hz).

magnitude nearly four times the final steady state current is generated (Fig. 10(a)). The transient current was insignificant when the phase difference is reduced to 10° (only the voltage criterion is violated). Fig. 10 indicates that there is no significant difference in the observed results between the forceful reconnection at 10° phase difference and the reconnection using synchrocheck relay (all criteria are satisfied). It should be noted that the final steady state current from the utility grid is reduced in the case where synchrocheck relay is used due to the switching of the capacitors. The peak transient current that is slightly higher than the case of forceful reconnection at 10° phase difference can also be attributed to the capacitor bank. The power outputs of the synchronous generator and the utility grid undergo few oscillations before reaching their respective steady state values (Fig. 10 (b)). However, power outputs of the VSC and induction generator do not show significant transient variations due to reconnection event in all three scenarios. The microgrid starts to export power to the utility grid after resynchronization. This happens due to the reduced load demand in the system with the load shedding in the islanded operation. Load restoration can be done once the system is stabilized (not shown in Fig. 10).

These results reveal that simple switched capacitor bank arrangement is sufficient to improve the voltage quality in islanded operation, although more sophisticated Var support schemes such SVCs, DSTATCOMS, energy storage systems or new control schemes are discussed in many studies [22–26]. The results also indicate that the synchronization criteria applied to individual distributed generators are satisfactory for microgrids of equivalent total generation. The effect of synchrocheck relay settings in applying for microgrid reconnection is further investigated in the next section.

5.3. Impact of synchrocheck relay settings

So far the settings of the synchrocheck relay were at the maximum allowed limits for DG interconnection [17] as illustrated

in Fig. 10. This section analyzes the impact of these settings on the microgrid synchronization performance.

The current frequency difference threshold is set at 0.1 Hz, which is the required limit for DGs greater than 1.5 MW capacity. This is also the steady state frequency deviation limit for distribution systems [6]. Therefore, it is desirable to leave the frequency difference threshold of synchrocheck relay at 0.1 Hz, even when applying to the MV microgrid of nearly 5 MW capacity considered in this study.

As observed in the results of Fig. 12, a lower phase difference shows a reduction in magnitudes of the current and power transients. Thus, it is desirable to set the phase angle difference threshold at the lowest possible value. The lowest possible threshold depends on the circuit breaker time delay and the slip-frequency, f_s (frequency difference between the microgrid and utility grid). The circuit breaker time delay considered in this study is 83 ms [45]. If $\Delta\phi_{th}$ is the phase difference threshold, and Δt_{insync} is the time duration that phase angle difference is within the threshold, the relationship between f_s (in Hz), $\Delta\phi_{th}$ (in degrees) and Δt_{insync} (in s) is given by [27]:

$$\Delta t_{insync} = \frac{\Delta\phi_{th}}{180f_s} \quad (3)$$

This Δt_{insync} should be greater than the circuit breaker time delay, which is 83 ms to ensure the microgrid reconnection within the set phase angle threshold. If $\Delta\phi_{th}$ is 10° then Δt_{insync} is 555 ms for the maximum possible slip frequency of 0.1 Hz. Similarly, if $\Delta\phi_{th}$ is set at 5° then, Δt_{insync} is 277 ms, which is still much higher than the circuit breaker time delay. Therefore, threshold for phase angle difference in synchronizing the microgrid can be brought down to 5° without any difficulty.

The threshold of voltage difference is currently set at 0.03 pu with a time delay of 5 s for the study. This time delay has to be maintained to avoid spurious switching during transients (the standards [6] requires this waiting time to be 5 min long, but 5 s delay is considered here to limit the simulation duration to a

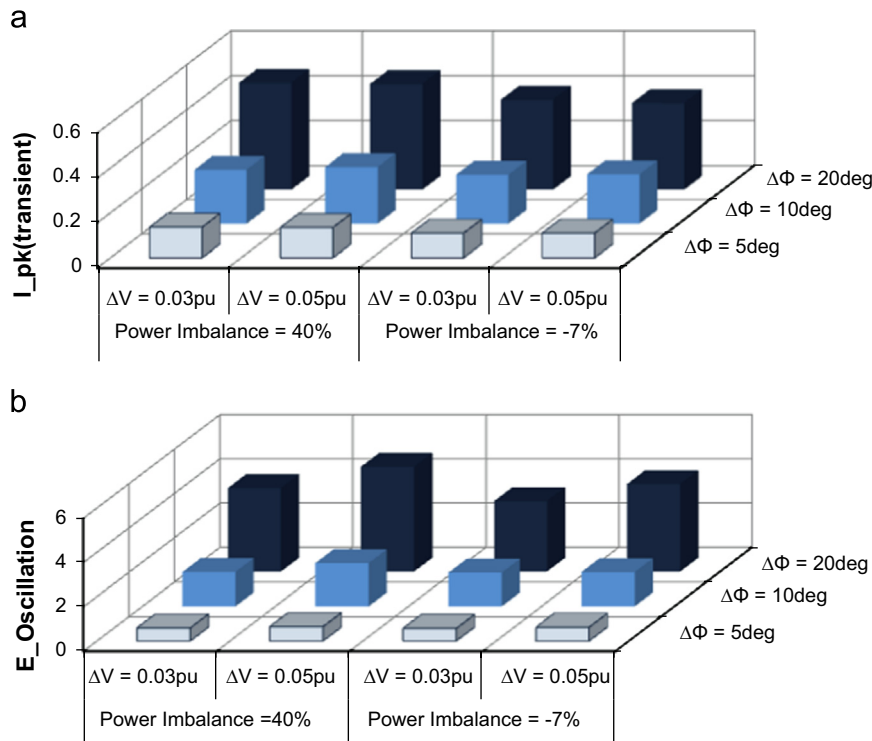


Fig. 12. (a) $I_{pk(transient)}$ (b) $E_{Oscillation}$ when microgrid is resynchronized to utility grid after islanding resulting in +40% and -7% power imbalance.

reasonable value). According to the distribution system standards, the steady state voltage magnitude deviation could be as large as $\pm 6\%$ from the nominal value [17]. Thus, the steady state voltage magnitude difference between the utility grid and microgrid could be larger than the difference specified in the synchronization requirements. In the microgrid simulation examples considered in Section 5.2, while in the islanded mode of operation, switched capacitors were applied to support the synchronization function. The capacitors were switched-in to meet the set voltage difference threshold of the synchrocheck relay. However, it is noticeable from Fig. 10 that the transient variations of the current (and power) following the reconnection in Scenarios 2 and 3 are not much different. (Since $\Delta\Phi_{th}$ was 10° for the synchrocheck relay, the difference between the two scenarios is the presence of the capacitor bank.) Therefore, it is explored whether the voltage difference threshold could be set to a higher value without undue effects. Such possibility would allow reducing the number of capacitor stages and switching operations.

To analyze the sensitivity of voltage difference threshold (ΔV_{th}), it is set to 0.03 pu and 0.05 pu keeping the frequency difference threshold (Δf_{th}) at 0.1 Hz. Three phase angle difference thresholds ($\Delta\Phi_{th}=5^\circ, 10^\circ$ and 20°) are considered. The capacitor switching voltage thresholds are adjusted as given in Table 5 so that the switching of the last set of capacitors results in voltage magnitudes that are just sufficient to meet the considered ΔV_{th} criteria (0.03 pu or 0.05 pu).

Fig. 11 presents the variation of phase-b grid current, voltage of the weakest bus (Bus-6), and real power outputs of all sources for an islanding event with +40% power imbalance and synchronizing it back to the utility grid after operating in the islanded mode for some duration. The results are shown for the case of $\Delta f_{th}=0.1$ Hz, $\Delta\Phi_{th}=10^\circ$ and $\Delta V_{th}=0.05$ pu.

With the aim of studying the effect of $\Delta\Phi_{th}$ and ΔV_{th} settings on smooth transition of microgrid from the islanded to parallel operation, two indicators are defined.

1. Peak transient current ($I_{pk(transient)}$) is the peak instantaneous transient current due to synchronizing operation. This is illustrated in Fig. 11(a)
2. Oscillation energy ($E_{oscillation}$) defined in (4) quantifies the oscillations in the utility active power due to synchronizing operation.

$$E_{oscillation} = |P_{pk(max)}| \times t_{settle} \quad (4)$$

where P_{pk} is the peak grid power observed during the initial oscillations following the synchronization, and t_{settle} is the oscillations settling time. These quantities are illustrated in Fig. 10(b).

These indicators are calculated using simulations for each of the cases described earlier [$\Delta f_{th}=0.1$ Hz, $\Delta V_{th}=0.03$ pu, 0.05 pu, and $\Delta\Phi_{th}=5^\circ, 10^\circ, 20^\circ$]. The microgrid resynchronizing after two different islanding events, resulting in -7% and $+40\%$ power imbalances, are studied.

Fig. 12(a) presents $I_{pk(transient)}$ under different scenarios described previously. It shows that initial current transient is significantly

large if $\Delta\Phi_{th}=20^\circ$. Current transient is reduced with the lower setting of the phase angle difference. Therefore, it is desirable to use a 5° phase angle threshold to achieve a comparatively low initial current transient at the POI, in reconnecting the microgrid back to the utility grid. At both power imbalances tested, it shows that there is no significant difference in using 0.03 pu or 0.05 pu as the voltage threshold. However, if $\Delta V_{th}=0.03$ pu, a larger capacitor bank is required at the POI to raise the voltage to meet the more strict voltage criterion.

Table 6 presents the total reactive power supplied at the POI by the switched capacitors for the two cases of $\Delta V_{th}=0.03$ pu and $\Delta V_{th}=0.05$ pu. When $\Delta V_{th}=0.05$ pu, the number of capacitor stages that need to be switched in has reduced. As a result, the current index values drop to half of those corresponding to $\Delta V_{th}=0.03$ pu. It should be noted that even though 0.05 pu voltage threshold reduces the required number of switched capacitor stages, the steady state voltage criteria specified in the standards [17] are not violated. For the -7% power imbalance case with $\Delta V_{th}=0.05$ pu, the maximum voltage deviation observed was -1.24% and the voltage unbalance was 0.58% in the islanded operation, which are well within the recommended values [17]. These observations suggest that relaxing the ΔV_{th} setting of the synchrocheck relay to 0.05 pu would not cause any power quality problems and helps in reducing the initial current transients at the POI.

Fig. 12(b) presents $E_{oscillation}$ values corresponding to the same conditions as in Fig. 12(a). Fig. 12(b) shows that the use of $\Delta\Phi_{th}=20^\circ$ resulted in significantly high oscillation energy index values (large and longer oscillations in grid power after synchronization). Decreasing the phase angle threshold from 10° to 5° reduced the oscillation energy index by a factor of three. This observation supported the previous discussions on setting the phase angle threshold of the synchro-check relay at the POI of microgrid at a value lower than the maximum permitted under the standards [6]. Simulation results in Fig. 12(b) also show that if the phase angle threshold is set below 10° , the $E_{oscillation}$ values remain nearly unchanged when the voltage threshold of the synchrocheck relay is increased from 0.03 pu to 0.05 pu, for both power imbalances simulated.

The total generation capacity of the microgrid test system considered in this paper is less than 5 MW, with a major portion (3 MW) coming from a synchronous generator. Voltage control and balancing during the islanded operation of the microgrid is achieved using a switched capacitor bank with automatic control. The simulation results presented in this paper suggest that for a MV microgrid with similar characteristics, the maximum voltage difference criteria for synchronization can be relaxed to 0.05 pu without undue effects, if the switchgear at the POI permits lowering the phase angle threshold below 10° (say to 5°). Relaxation of the voltage threshold criteria helps reducing the number of capacitor bank stages used for voltage support (and balancing) and thereby lowering the capacitor inrush currents. This reduces the magnitude of the current transient observed during the synchronization and ensures a seamless transition from islanded to parallel operation while satisfying the steady state voltage limits specified in standards during both parallel and islanded operation.

Table 5

Capacitor switching criteria set at different voltage difference thresholds of the synchrocheck relay.

Switches	Time delay (s)	Voltage setting for capacitor switching (pu)	
		$\Delta V_{th}=0.03$ pu	$\Delta V_{th}=0.05$ pu
S1a, S1b, S1c	6	0.985	0.965
S2a, S2b, S2c	4	0.980	0.960
S3a, S3b, S3c	2	0.975	0.955

Table 6

Reactive power injection at POI at different ΔV_{th} .

Case	Total reactive power injection at POI (kVar)	
	$\Delta V_{th}=0.03$ pu	$\Delta V_{th}=0.05$ pu
40% Power imbalance	450	150
-7% Power imbalance	750	600

6. Conclusions

This paper reviewed the techniques available for synchronization of islanded microgrids and the applicable international standards that guide the synchronization process. The literature review revealed that most practical microgrids with inverter based DGs use active synchronization; and that the published information on passive synchronization of microgrids with more than one generator is limited. The process of passive synchronization with traditional synchrocheck relays was examined in detail through a simulated microgrid test system with highly unbalanced loading and different types of generation. The paper also examined the application of switched capacitor banks for voltage balancing in an islanded microgrid for achieving the voltage magnitude criteria for synchronization. The findings show that with simple switched capacitors at the POI, it is possible to meet the voltage quality of the microgrid and synchronization requirements specified in the standards. In microgrid synchronization, the major factor that determines the smooth transition was the phase angle difference between the utility and microgrid voltages. The results also show that, when switched capacitors are used at the POI, it is desirable to relax the voltage difference threshold of the synchrocheck relay to reduce the initial current transients during the reconnection of the microgrid to the utility grid. It can also be concluded that the traditional synchrocheck relays are quite satisfactory for microgrid synchronization.

Acknowledgements

The authors acknowledge the support given by Corey Senkow, Distributed Resources Interconnection Engineer, Manitoba Hydro, Winnipeg, MB, Canada, and Dharshana Muthumuni, Manitoba HVDC Research Centre, Winnipeg, MB, Canada.

References

- [1] Hart DG, Kunsman SA, Luyster B. Microgrids—integrating renewable energy sources (RES) to improve reliability. *PAC World* 2013;25:54–9 (Sep.).
- [2] Jenkins N, Allan R, Crossley P, Kirschen D, Strbac G. Embedded generation, UK: IEE; 2000.
- [3] Chowdhury S, Chowdhury SP, Crossley P. Microgrids and active distribution networks, IET Renewable Energy Series 6, UK: IET; 2009.
- [4] Lidula NWA, Rajapakse AD. Microgrids research: a review of experimental microgrids and test systems. *Renewable Sustainable Energy Rev J* 2011;15: 186–202.
- [5] Guide for design, operation, and integration of distributed resource island systems with electric power systems. IEEE STD 1547.4-2011.
- [6] Interconnecting distributed resources with electric power systems, IEEE Standard 1547-2003.
- [7] Cho C, Jeon Jin-Hong, Kim Jong-Yul, Kwon S, Park K, Kim S. Active synchronizing control of a microgrid. *IEEE Trans Power Electron* 2011;26(12):3707–18.
- [8] Kroposki B, Pink C, Lynch J, John V, Daniel SM, Benedict E, et al. Development of a high-speed static switch for distributed energy and microgrid applications. *PCC* 2007;1418–23.
- [9] Lasseter RH, Piagi P. Control and design of microgrid components, final project report: PSERC publication 06-03; Jan 2006.
- [10] Yazdani Davood, Bakhshai Alireza, Joos Geza, Mojiri M. A nonlinear adaptive synchronization technique for grid-connected distributed energy sources. *IEEE Trans Power Electron* 2008;23(4):2181–6.
- [11] Majumder R, Ghosh A, Ledwich G, Zare F. Power management and power flow control with back-to-back converters in a utility connected microgrid. *IEEE Trans Power Syst* 2010;25(2):821–34.
- [12] Lee Chia-Tse, Jiang Ruei-Pei, Cheng Po-Tai. A grid synchronization method for droop-controlled distributed energy resource converters. *IEEE Trans Ind Appl* 2013;49(2):954–62.
- [13] Guerrero Josep M, Vazquez Juan C, Matas José, García de Vicuña Luis, Castilla Miguel. Hierarchical control of droop-controlled ac and dc microgrids—a general approach toward standardization. *IEEE Trans Ind Electron* 2011;58(1):158–72.
- [14] Rocabert Joan, Azevedo Gustavo MS, Luna Alvaro, Guerrero Josep M, Ignacio Candela Jose, Rodríguez Pedro. Intelligent connection agent for three-phase grid-connected microgrids. *IEEE Trans Power Electron* 2011;26(10):2993–3005.
- [15] Vandoorn Tine L, Meersman Bart, Kooning Jeroen DM De, Vandevelde Lieven. Transition from islanded to grid-connected mode of microgrids with voltage-based droop control. *IEEE Trans Power Syst* 2013;28(3):2545–53.
- [16] Bellini A, Bifaretti S, Giannini F. A robust synchronization method for centralized microgrids. In: IEEE energy conversion congress and exposition (ECCE); 2013. p. 4587–4594.
- [17] Technical requirements for connecting distributed resources to the Manitoba Hydro system, DRG 2003, Rev2, MBHydro Electric Board; 2010.
- [18] ABB, Synchrocheck relay, product guide SPAU 140 C, 1MRS750421-MBG, Ver: C/25.04.2006; 2006.
- [19] Synchronism check relays, MIJ, instructions manual, GEK-106213C, GE Power Management. Available at: <http://www.gedigitalenergy.com/products/manuals/mlj/mljman-c.pdf>.
- [20] Laaksonen H, Kauhaniemi K. Synchronized re-connection of island operated a LV microgrid back to utility grid. In: Innovative smart grid technologies conference Europe (ISGT Europe); 2010. IEEE PES. p. 1–8.
- [21] Lessa Assis Tatiana Mariano, Taranto Glauco Nery. Automatic reconnection from intentional islanding based on remote sensing of voltage and frequency signals. *IEEE Trans Smart Grid* 2012;3(4):1877–84.
- [22] Sao C, Lehn PW. Voltage balancing of converter fed microgrids with single phase loads. In: Power and energy society general meeting—conversion and delivery of electrical energy in the 21st Century; 2008. IEEE. p. 1–7.
- [23] Vandoorn TL, Renders B, Degroote L, Meersman B, Vandevelde L. Power balancing in islanded microgrids by using a dc-bus voltage reference. In: International symposium on power electronics electrical drives automation and motion (SPEEDAM); 2010. p. 884–889.
- [24] Rezaei E, Afsharnia S. Cooperative voltage balancing in islanded microgrid with single-phase loads. In: International conference on electrical and control engineering (ICECE); 2011. p. 5804–5808.
- [25] Lee Tzung-Lin Hu, Shang-Hung Chan, Yu-Hung. Design of D-STATCOM for voltage regulation in microgrids. In: energy conversion congress and exposition (ECCE); 2010. IEEE. p. 3456–3463.
- [26] Bogóñez-Franco P, Balcells J, Junyent O, Jordà J. SVC model for voltage Control of a microgrid. In: IEEE international symposium on industrial electronics (ISIE); 2011. p. 1645–1649.
- [27] Joseph E, Lasseter R, Schenkman B, Stevens J, Volkammer H, Klapp D, et al. CERTS microgrid laboratory Testbed. Consortium for electric reliability technology solutions (CERTS), California Energy Commission, Public Interest Energy Research Program, CEC-500-2008-XXX; 2008.
- [28] Hatta H, Kobayashi H. A study of centralized voltage control method for distribution system with distributed generation. In: International conference on electricity distribution; 2007. Paper 0330.
- [29] Hirose K, Takeda T, Muroyama S. Study on field demonstration of multiple power quality levels system in Sendai. In: INTELEC '06, telecommunications energy conference, IEEE; 2006. p. 1–6.
- [30] Katiraei F, Abbey C, Tang S, Gauthier M. Planned islanding on rural feeders—utility perspective. In: Invited paper for presentation at the IEEE PES general meeting (panel on microgrids); 2008. p. 1–6.
- [31] CIGRE C6.04.02 Task Force, Benchmark modeling and simulation for analysis, design, and validation of distributed energy systems; Sep 2006.
- [32] PSCAD online help system, Manitoba HVDC Research Center Inc., MB, Canada; 2003–2006.
- [33] Etxegarai A, Eguía P, Zamora I. Analysis of remote islanding detection methods for distributed resources. In: International conference on renewable energies and power quality (ICREPQ'11); April 2011.
- [34] Lidula NWA, Rajapakse A. A pattern recognition approach for detecting power islands using transient signals—Part I: Design and implement. *IEEE Trans Power Delivery* 2010;25(4):3070–7.
- [35] Kundur P. Power system stability and control. USA: McGraw-Hill; 1994.
- [36] Anderson PM, Bose A. Stability simulation of wind turbine systems. *Trans Power Appa Syst* 1983;102(12):3791–5 (Dec).
- [37] Arrillaga J, Liu YH, Watson NR. Flexible power transmission, the HVDC options. UK: John Wiley & Sons Ltd; 2007.
- [38] Suh Y, Tijeras V, Lipo TA. A nonlinear control of the instantaneous power in dq synchronous frame for PWM AC/DC converter under generalized unbalanced operating conditions. In: 37th IAS annual meeting; 2002. vol. 2, p. 1189–1196.
- [39] Moustafa MMZ, Filizadeh S. Simulation of a VSC transmission scheme supplying a passive load. In: Industrial electronics. IECON 2008. 34th Annual conference of IEEE; 2008.
- [40] GE power management. Load shedding, load restoration and generator protection using solid-state and electromechanical under frequency relays, Ontario, Canada, Rep. GET-6449.
- [41] Zin AAM, Hafcz HM, Wong WK. Static and dynamic under-frequency load shedding: a comparison. In: Proceedings of international conference on power system tech. POWERCON 2004, Singapore; 2004. vol. 1, p. 941–945.
- [42] Transend Networks Pty Ltd, Frequency Standard Development, final report to Alinta Power, TrimD07:66728; Dec 2007.
- [43] Delfino B, Massucco S, Morini A, Scalera P, Silvestro F. Implementation and comparison of different under frequency load-shedding schemes. In: PES Summer Meeting; 2001. IEEE, vol. 1, p. 307–312.
- [44] Network planning guideline for MV shunt capacitors, guideline, Eskom Distribut Tech, revised on; June 2010. Available at: <http://bits.eskom.co.za/dtechsec/distribut/tech/GUIDE/DGL-34-598.pdf>.
- [45] Specification of FRANKE's MV capacitor banks and capacitors, FrankeGmkp Energy Ltd. Available at: <http://www.frankeenergy.com/84.pdf>.